ChemComm

Heteroleptic copper(I) charge-transfer chromophores with panchromatic absorption

Journal:	*ChemComm*
Manuscript ID	CC-COM-07-2022-003873.R2
Article Type:	Communication

COMMUNICATION

Heteroleptic copper(I) charge-transfer chromophores with panchromatic absorption

Dooyoung Kim,[a] Thomas G. Gray,[b] and Thomas S. Teets*[a]

Received 00th January 20xx,
Accepted 00th January 20xx

DOI: 10.1039/x0xx00000x

Four new heteroleptic bis-chelate Cu(I) complexes showing panchromatic visible absorption are described here. With this heteroleptic design, we demonstrate that the energy levels of the spatially separated HOMO and LUMO can be independently and systematically controlled via ligand modification, with charge-transfer absorption bands throughout the visible and NIR regions that cover a wider range than typical Cu(I) chromophores.

In the field of solar photochemistry, harvesting solar energy and converting it to a chemical potential is critically important. Since molecular photosensitizers can absorb visible light and transfer excited-state energy and/or charge, they have been widely used in photochemistry applications including solar fuels[1,2] and dye-sensitized solar cells.[3] Outside of these solar energy-related areas, researchers in the organic synthesis field have exploited molecular photosensitizers as powerful tools to carry out challenging organic reactions under mild conditions.[4,5]

The most widely used molecular photosensitizers are precious-metal complexes based on ruthenium[6] or iridium.[7] Due to the high-price and scarcity of precious metals, cheaper alternatives such as metal-free organic photosensitizers[8–10] or earth-abundant transition metal-based photosensitizers[11–13] have emerged for more sustainable development of large-scale applications. 3*d* photosensitizers present specific technical challenges; those with partially filled d orbitals have low-lying ligand-field (*d*–*d*) excited states[14] that can deactivate the desired charge-transfer excited state. One approach to relieve this problem is to use d^0 or d^{10} transition metals such as Zr(IV)[15] or Cu(I)[16]

The most common Cu(I) photosensitizers are $[Cu(phen^R)_2]^+$, where phen^R is a substituted 1,10-phenanthroline. When these D_{2d}-symmetric Cu(I) complexes undergo metal-to-ligand charge transfer (MLCT) excitation, the copper center has a formal +2 oxidation state and is Jahn-Teller-active,[17–19] leading to a flattening distortion that reduces the excited-state lifetime. The widespread solution to this challenge has been to incorporate bulky substituents onto the 2- and 9-positions of the phenanthroline to sterically block this distortion.[20–22] Another approach is to synthesize heteroleptic Cu(I) complexes using diphosphine ligands in combination with phen^R derivatives.[23] These compounds can have very long excited-state lifetimes, but they typically absorb very poorly in the visible region. Some metal complexes with panchromatic absorption using π-extended and/or π-donating chelating ligands have been studied, primarily with group 8 transition metals.[24–29]

In this work we introduce a new class of charge-neutral heteroleptic Cu(I) chromophores, pairing 1,10-phenanthroline (phen) and 2,2′-biquinoline (biq) neutral diimine ligands (N^N) with variably substituted, anionic β-diketiminate (NacNac^R) ligands. Related compounds have been disclosed, focusing mainly on structural aspects.[30] The design introduced here borrows insights from our previous work on Ir(III) photosensitizers supported by NacNac^R ligands, which showed that the HOMO is mainly localized on NacNac^R,[31] and its energy is tuned by modifying substituents on the NacNac^R.[31,32] These Ir(III) photosensitizers are potent photoreductants and are effective in organic synthesis applications.[34,35] Unlike traditional $[Cu(phen^R)_2]^+$ complexes, where the HOMO (mixed Cu/N^N orbital) and LUMO (N^N π* orbital) are strongly coupled,[33,34] the frontier orbitals in the reported Cu(N^N)(NacNac^R) heteroleptic compounds can be independently controlled, allowing the HOMO–LUMO gap and corresponding charge-transfer absorption band to be readily tuned by simple synthetic modifications of each ligand.

The syntheses of four Cu(N^N)(NacNac^R) complexes and their chemical structures are outlined in Scheme 1, together with their numerical designations. All Cu(I) complexes were prepared by stirring equimolecular amounts of CuO^{t}Bu and the protonated β-diketiminate NacNac^R(H) first, then adding 1 equiv. of diimine ligand (N^N) in toluene solution at room temperature or with mild heating. The Cu(I) complexes were isolated in 19–57% yield and characterized by multi-nuclear NMR (Fig. S16–S23 in the ESI†). All complexes are air- and moisture-sensitive. However, they are reasonably photostable,

[a] *Department of Chemistry, University of Houston, 3585 Cullen Blvd. Room 112, Houston, TX, 77204-5003, USA. E-mail: tteets@uh.edu*
b Department of Chemistry, Case Western Reserve University, Cleveland, OH, 44106, USA.

† Electronic Supplementary Information (ESI) available: Experimental details, X-ray crystallography summary tables, cyclic voltammograms, NMR spectra, DFT results, and DFT output files in .xyz format. CCDC 2179415–2179418 contain the crystallographic data. See DOI: 10.1039/x0xx00000x

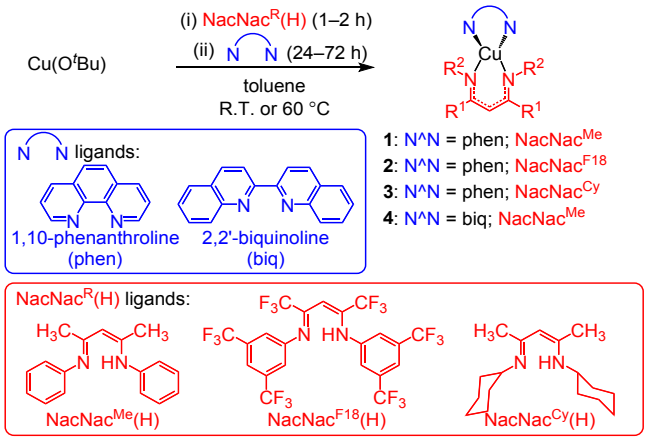

Scheme 1. Synthesis of heteroleptic Cu(N^N)(NacNac^{R}) complexes.

with no new diamagnetic products appearing over 48 hours of irradiation with blue LEDs in C_6D_6 under nitrogen atmosphere (Fig. S7–S10 in the ESI†). The molecular structures of all complexes, determined by single-crystal X-ray diffraction, are shown in Fig. 1 and the refinement data are summarized in Tables S1 and S2 of the ESI.† Crystal structures reveal the heteroleptic bis-chelate nature of Cu(I) complexes, with near C_{2v} symmetry. The structures of these compounds were further evaluated by determining τ_4 and τ_δ geometric indices.[35,36] As presented in Table S7, τ_4 ranges from 0.69 to 0.81 and τ_δ ranges from 0.65 to 0.78, indicating distorted tetrahedral structures. In the crystal structure of **1**, the phenanthroline ligand is tilted relative to the NacNac^{Me} due to intermolecular π-stacking interactions involving phen ligands on adjacent molecules, with a centroid-to-centroid distance of 3.39 Å (Fig. S1 in the ESI†). This structural distortion is relaxed in solution, as determined by comparing the solid-state structure with the DFT geometry optimization in toluene solution (Fig. S2). Larger τ_4 and τ_δ values are observed from the DFT-optimized structure (τ_4 = 0.77, τ_δ = 0.76) compared to the crystal structure (τ_4 = 0.69, τ_δ = 0.65) (Table S7).

The frontier orbital energy levels of all complexes were computed by DFT and experimentally evaluated via cyclic voltammetry (Fig. 2). Kohn–Sham frontier orbital depictions for **1–4** with partial orbital energy-level diagrams are presented in Fig. S11–S14 of the ESI†, with HOMO and LUMO levels summarized in Fig. 2. The LUMO in these complexes is mainly localized on the diimine ligand (94%–96% of density for phen complexes **1–3**, and 92% for biq complex **4**) and the HOMO is delocalized between Cu and the NacNac^{R} ligand. As the electron-richness of the NacNac^{R} increases (NacNac^{Cy} > NacNac^{Me} > NacNac^{F18}), the HOMO becomes more NacNac-localized (79% on NacNac^{Cy} for **3**, 54% on NacNac^{Me} for **1**, and 37% on NacNac^{F18} for **2**). Comparing the Cu(phen)(NacNac^{R}) series (**1–3**), the LUMO energies span a small range of about 0.4 eV, from −2.34 eV (NacNac^{F18} complex **2**) to −1.91 eV (NacNac^{Cy} complex **3**). In contrast, the HOMO energies are strongly responsive to the NacNac^{R} substitution pattern, spanning a 1.3 eV range from −5.62 eV (NacNac^{F18}) to −4.32 eV (NacNac^{Cy}). The two Cu(N^N)(NacNac^{Me}) complexes (**1** and **4**) show that the LUMO energy is substantially shifted by altering the N^N ligand, with minimal effect on the HOMO energy. Replacing phen (**1**) with biq (**4**) stabilizes the LUMO energy by 0.45 eV with the

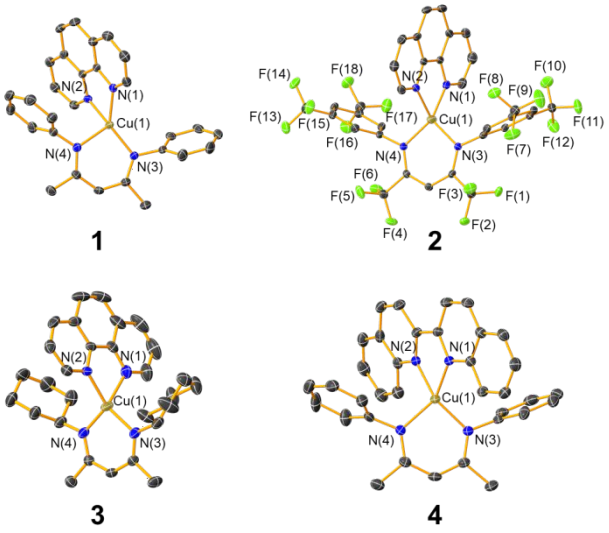

Fig. 1. Molecular structures of **1–4** determined by single-crystal X-ray diffraction. Thermal ellipsoids are drawn at the 50% probability level and hydrogen atoms are omitted for the clarity.

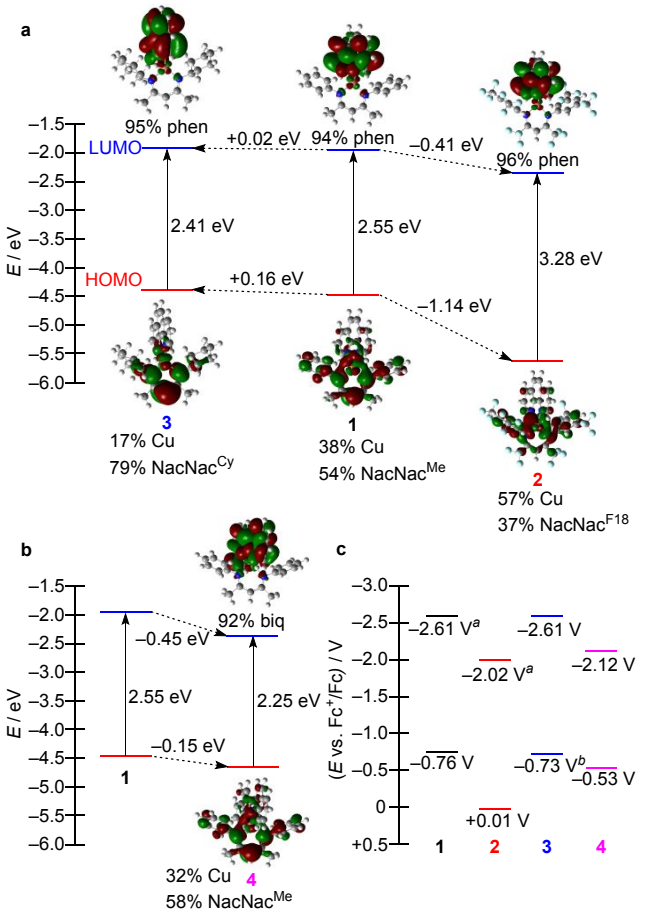

Fig. 2. Frontier orbital energy levels and compositions of complexes a) Cu(phen)(NacNac^{R}) and b) Cu(N^N)(NacNac^{Me}) complexes, determined by DFT with implicit toluene solvation. Orbital percentages are as a function of density. c) Redox potentials of complexes **1–4** determined by cyclic voltammetry. For irreversible waves, ^{a} cathodic ($E_{p,c}$) or ^{b} anodic ($E_{p,a}$) peak potentials are reported.

HOMO decreasing only by 0.15 eV, demonstrating the independent tunability of HOMO and LUMO energy levels.

The redox potentials of **1–4** determined by cyclic voltammetry are presented in Fig. 2c and summarized in Table 1, and the voltammograms are shown in Fig. S15 of the ESI.† The electrochemical data reproduce the trends observed by DFT. Unlike most Cu(I) diimine complexes which have oxidation potentials more positive than the ferrocene couple ($Fc^{+/0}$),[22,37,38] **1–4** have oxidation waves at or below the ferrocene couple, formally Cu^{II}/Cu^{I} but also involving substantial $NacNac^{R}$ oxidation based on the computed HOMO composition (see Fig. 2 and above discussion). This large potential shift relative to homoleptic copper diimine complexes is a result of the electron-rich, π-donating NacNac ligand, which destabilizes the HOMO. The oxidation wave is strongly responsive to the $NacNac^{R}$ substitution pattern, for example anodically shifting by about 700 mV from **1** ($NacNac^{Me}$) to **2** ($NacNac^{F18}$), which is decorated with electron-withdrawing groups. Replacement of the *N*-phenyl rings (**1**) with cyclohexyl groups (**3**) leads to a slight cathodic shift of the anodic peak potential ($E_{p,a}$) by 60 mV, indicating the more electron-rich $NacNac^{Cy}$ destabilizes the HOMO. The complexes also show cathodic waves in their CVs, indicating reduction of the complex via population of the N^N π* LUMO. In the Cu(phen)($NacNac^{R}$) series (**1–3**), the differences in reduction potential are smaller than the differences in the above-mentioned oxidation wave. Altering the diimine ligand in the two Cu(N^N)($NacNac^{Me}$) (**1** and **4**) has a large effect on the reduction potential, with the reduction potential of **4** (−2.12 V) more positive than that of **1** (−2.61 V) by 490 mV. In contrast, the difference between the oxidation potentials of those two complexes is only 230 mV. Therefore, the electrochemical data further demonstrate that the spatially separated HOMO and LUMO can be independently tuned by altering the $NacNac^{R}$ and N^N ligands, respectively.

UV–vis absorption spectra of **1–4** are overlaid in Fig. 3 and the data summarized in Table 1. All the complexes exhibit intense ligand-centered π→π* transitions in the UV region (λ < 350 nm) and broad, low-energy charge-transfer bands that span the visible to near-infrared region. Complexes **1** and **3** with electron-rich NacNac ligands exhibit broad low-energy charge-transfer bands that result in panchromatic visible absorption. Molar absorptivity (ε) values of these intense charge-transfer bands are on the order of 10^3 $M^{-1}cm^{-1}$. The peak wavelengths

Table 1. Summary of photophysical and electrochemical data. UV-vis data was measured toluene, electrochemical data in THF with 0.1 M NBu_4PF_6 supporting electrolyte.

	λ / nm ($\varepsilon\times10^{-3}$ / $M^{-1}cm^{-1}$)	E^{ox} / V	E^{red} / V
1	351[a] (23), 396 (17), 634 (4.5)	−0.76	−2.61[b]
2	323 (33), 489 (7.3)	+0.01	−2.02[b]
3	374 (5.8), 696 (3.4)	−0.73[c]	−2.61
4	314 (35), 326 (38), 340 (37), 356[a] (24), 420[a] (6), 796 (1.9)	−0.53	−2.12

[a] shoulder [b] Irreversible wave. Cathodic peak potential ($E_{p,c}$) is indicated. [c] Irreversible wave. Anodic peak potential ($E_{p,a}$) is indicated.

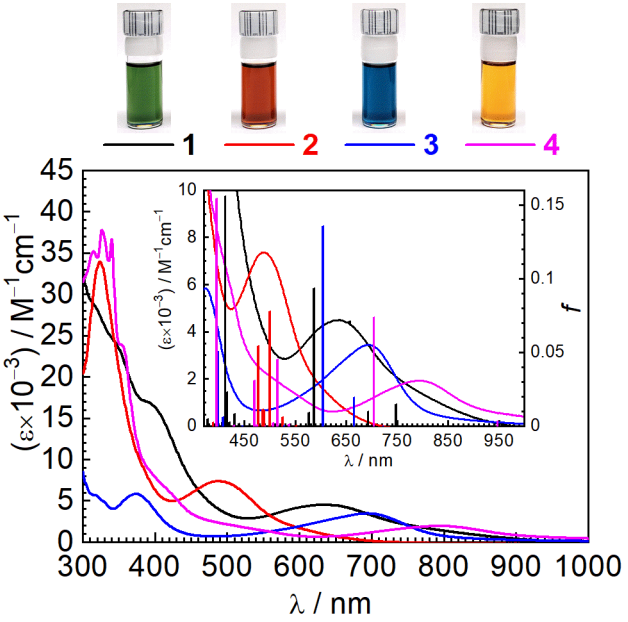

Fig. 3. Overlaid UV–vis absorption spectra of complexes **1–4**, obtained in toluene at room temperature (Black: **1**, Red: **2**, Blue: **3**, Magenta: **4**). The low-energy charge-transfer bands in the visible and near-infrared regions are presented in the inset. The vertical lines in the inset are calculated transition wavelengths and corresponding oscillator strengths, determined by TD-DFT with implicit toluene solvation. The photographs above the plot show toluene solutions of the complexes at concentrations of ca. 0.3 mM.

of the low-energy charge-transfer absorption bands correlate with the HOMO–LUMO gaps estimated by DFT calculations and cyclic voltammetry (Fig. 2). The charge-transfer maxima of **1** and **3** are 634 nm and 696 nm, respectively, whereas **2** displays a corresponding band at shorter wavelength, 489 nm, on account of the stabilized HOMO and larger HOMO–LUMO gap. Replacing phen with biq stabilizes the LUMO and gives a smaller HOMO–LUMO gap and red-shifted charge-transfer absorption. Complex **4** (N^N = biq) has a low-energy absorption band centered at 796 nm, a much longer wavelength than that of **1** (634 nm).

Calculated singlet transitions and oscillator strengths determined by TD-DFT are overlaid with experimental UV–vis absorption spectra in the inset of Fig. 3 and comprehensively summarized in Tables S8–S11 of the ESI†. Experimentally we observe a decrease in ε as the charge-transfer band shifts to lower energy, although the trend in oscillator strengths (*f*) is not as clear in the TD-DFT. Nevertheless, the low-energy charge-transfer excitation consists of overlapping transitions involving primarily HOMO–1 and HOMO as the donor orbitals and the LUMO and LUMO+1 as acceptor orbitals. All transitions with significant oscillator strength involve two one-electron transitions mixing through configuration interaction. When considering the nature of the frontier orbitals as shown in Fig. 2 and summarized in Tables S8–S11, these low-energy transitions can be assigned as mixed metal-ligand to ligand charge transfer (MMLL'CT), intermediate between metal-to-ligand charge transfer (MLCT) and ligand-to-ligand charge transfer (LL'CT). As illustrated in Fig. 2, the HOMO of **2** is more localized on the metal, and the low-energy charge-transfer band thus has more MLCT character. Complexes **1**, 3, and **4** have more electron-rich

NacNac^R ligands with HOMO is more NacNac^R-localized, leading to greater LL'CT character in the absorption band.

Complexes **1–4** are not luminescent in solution at room temperature or 77 K, and preliminary investigations of hydrodehalogenation and ketone reduction photoredox reactions using these complexes as photosensitizers were unsuccessful. We suspect the lack of luminescence and photoredox reactivity indicates short excited-state lifetimes in these compounds, so a major goal moving forward is to discover molecular design strategies that beget longer charge-transfer lifetimes and lead to luminescence and/or productive charge transport following solar excitation.

In summary, four heteroleptic bis-chelate Cu(I) chromophores have been prepared and characterized. We demonstrate that the HOMO and LUMO energies of these complexes here are independently tunable by simple modification of ligand substituents, due to their spatially separated frontier orbitals. These chromophores show strong absorption spanning the UV, visible, and near-infrared regions, including intense charge-transfer bands that span a much larger portion of the spectrum than typical copper photosensitizers.

T.S.T. acknowledges the Welch Foundation (E-1887) and the University of Houston, through the High Priority Area Research Seed Grants, for funding this work. T.G.G acknowledges the Office of Naval Research for funding (ONR; Contract N00014-21-1-2230).

Author Contributions

Dooyoung Kim: conceptualization, formal analysis, investigation, validation, visualization, writing – original draft. Thomas G. Gray: conceptualization, formal analysis, funding acquisition, investigation, visualization, writing – review & editing. Thomas S. Teets: conceptualization, funding acquisition, project administration, visualization, writing – review & editing.

Conflicts of interest

There are no conflicts to declare.

Notes and references

1 T. S. Teets and D. G. Nocera, *Chem. Commun.*, 2011, **47**, 9268.
2 T. R. Cook, D. K. Dogutan, S. Y. Reece, Y. Surendranath, T. S. Teets and D. G. Nocera, *Chem. Rev.*, 2010, **110**, 6474–6502.
3 J.-F. Yin, M. Velayudham, D. Bhattacharya, H.-C. Lin and K.-L. Lu, *Coord. Chem. Rev.*, 2012, **256**, 3008–3035.
4 A. Pannwitz and O. S. Wenger, *Chem. Commun.*, 2019, **55**, 4004–4014.
5 N. Holmberg-Douglas and D. A. Nicewicz, *Chem. Rev.*, 2022, **122**, 1925–2016.
6 J. M. R. Narayanam and C. R. J. Stephenson, *Chem Soc Rev*, 2011, **40**, 102–113.
7 C. K. Prier, D. A. Rankic and D. W. C. MacMillan, *Chem. Rev.*, 2013, **113**, 5322–5363.
8 B. Zilate, C. Fischer and C. Sparr, *Chem. Commun.*, 2020, **56**, 1767–1775.
9 Q.-F. Bao, Y. Xia, M. Li, Y.-Z. Wang and Y.-M. Liang, *Org. Lett.*, 2020, **22**, 7757–7761.
10 A. Bhattacherjee, M. Sneha, L. Lewis-Borrell, G. Amoruso, T. A. A. Oliver, J. Tyler, I. P. Clark and A. J. Orr-Ewing, *J. Am. Chem. Soc.*, 2021, **143**, 3613–3627.
11 L. A. Büldt and O. S. Wenger, *Angew. Chem. Int. Ed.*, 2017, **56**, 5676–5682.
12 A. Aydogan, R. E. Bangle, A. Cadranel, M. D. Turlington, D. T. Conroy, E. Cauët, M. L. Singleton, G. J. Meyer, R. N. Sampaio, B. Elias and L. Troian-Gautier, *J. Am. Chem. Soc.*, 2021, **143**, 15661–15673.
13 D. Hong, Y. Tsukakoshi, H. Kotani, T. Ishizuka and T. Kojima, *J. Am. Chem. Soc.*, 2017, **139**, 6538–6541.
14 J. K. McCusker, *Science*, 2019, **363**, 484–488.
15 Y. Zhang, T. S. Lee, J. L. Petersen and C. Milsmann, *J. Am. Chem. Soc.*, 2018, **140**, 5934–5947.
16 H. Takeda, Y. Monma and O. Ishitani, *ACS Catal.*, 2021, **11**, 11973–11984.
17 D. R. Crane, J. DiBenedetto, C. E. A. Palmer, D. R. McMillin and P. C. Ford, *Inorg. Chem.*, 1988, **27**, 3698–3700.
18 M. Iwamura, S. Takeuchi and T. Tahara, *J. Am. Chem. Soc.*, 2007, **129**, 5248–5256.
19 J. R. Miecznikowski, M. A. Lynn, J. P. Jasinski, E. Reinheimer, D. W. Bak, M. Pati, E. E. Butrick, A. E. R. Drozdoski, K. A. Archer, C. E. Villa, E. G. Lemons, E. Powers, M. Siu, C. D. Gomes and K. N. Morio, *J. Coord. Chem.*, 2014, **67**, 29–44.
20 M. W. Mara, K. A. Fransted and L. X. Chen, *Coord. Chem. Rev.*, 2015, **282–283**, 2–18.
21 M. Y. Livshits, B. J. Reeves, N. J. DeWeerd, S. H. Strauss, O. V. Boltalina and J. J. Rack, *Inorg. Chem.*, 2020, **59**, 2781–2790.
22 M. C. Rosko, K. A. Wells, C. E. Hauke and F. N. Castellano, *Inorg. Chem.*, 2021, **60**, 8394–8403.
23 C. Minozzi, A. Caron, J.-C. Grenier-Petel, J. Santandrea and S. K. Collins, *Angew. Chem. Int. Ed.*, 2018, **57**, 5477–5481.
24 J. D. Braun, I. B. Lozada and D. E. Herbert, *Inorg. Chem.*, 2020, **59**, 17746–17757.
25 Z. Tang, X.-Y. Chang, Q. Wan, J. Wang, C. Ma, K.-C. Law, Y. Liu and C.-M. Che, *Organometallics*, 2020, **39**, 2791–2802.
26 A. Bessette, M. Cibian, J. G. Ferreira, B. N. DiMarco, F. Bélanger, D. Désilets, G. J. Meyer and G. S. Hanan, *Dalton Trans.*, 2016, **45**, 10563–10576.
27 G. Li, L. Ray, E. N. Glass, K. Kovnir, A. Khoroshutin, S. I. Gorelsky and M. Shatruk, *Inorg. Chem.*, 2012, **51**, 1614–1624.
28 R. Juwita, J.-Y. Lin, S.-J. Lin, Y.-C. Liu, T.-Y. Wu, Y.-M. Feng, C.-Y. Chen, H.-H. Gavin Tsai and C.-G. Wu, *J. Mater. Chem. A*, 2020, **8**, 12361–12369.
29 S. Lazic, P. Kaspler, G. Shi, S. Monro, T. Sainuddin, S. Forward, K. Kasimova, R. Hennigar, A. Mandel, S. McFarland and L. Lilge, *Photochem. Photobiol.*, 2017, **93**, 1248–1258.
30 P. O. Oguadinma, A. Rodrigue-Witchel, C. Reber and F. Schaper, *Dalton Trans.*, 2010, **39**, 8759–8768.
31 J.-H. Shon and T. S. Teets, *Inorg. Chem.*, 2017, **56**, 15295–15303.
32 J.-H. Shon, D. Kim, M. D. Rathnayake, S. Sittel, J. Weaver and T. S. Teets, *Chem. Sci.*, 2021, **12**, 4069–4078.
33 C. C. Phifer and D. R. McMillin, *Inorg. Chem.*, 1986, **25**, 1329–1333.
34 R. M. Everly and D. R. McMillin, *J. Phys. Chem.*, 1991, **95**, 9071–9075.
35 L. Yang, D. R. Powell and R. P. Houser, *Dalton Trans*, 2007, 955–964.
36 M. H. Reineke, M. D. Sampson, A. L. Rheingold and C. P. Kubiak, *Inorg. Chem.*, 2015, **54**, 3211–3217.
37 C. E. McCusker and F. N. Castellano, *Inorg. Chem.*, 2013, **52**, 8114–8120.
38 L. Kohler, R. G. Hadt, D. Hayes, L. X. Chen and K. L. Mulfort, *Dalton Trans*, 2017, **46**, 13088–13100.

